

Optimizing dynamic response and stability of pressure-controlled swash plate type axial piston pump

Vivek Verma¹, Sachin Kumar², Apurva Anand³

¹Department of Mechanical Engineering, Amity School of Engineering and Technology, Amity University, Lucknow, India

²Department of Electronics and Communication Engineering, Amity School of Engineering and Technology, Amity University, Lucknow, India

³Shri Ramswaroop Memorial University, Lucknow, India

Article Info

Article history:

Received May 9, 2024

Revised Sep 19, 2024

Accepted Sep 30, 2024

Keywords:

Gain margin

Lag-lead compensator

Phase margin

Pressure-controlled pump

Steady-state response

Transient response

VAPP

ABSTRACT

The main objective of the paper is to explore the role of lead-lag compensators in improving the performance of control systems for variable delivery hydraulic axial piston pumps (VAPP). These compensators offer a range of benefits, including stability enhancement, transient response optimization, frequency response modification, disturbance rejection, and robustness improvement. A mathematical model of the hydro-mechanical system is developed, and the transfer function for the dynamic system is established. The simulation of the model with lead-lag compensator significantly enhanced the phase margin to 55.7° and gain margin to 12.3 dB ensuring robust control for pressure-controlled VAPP, whereas the uncompensated system is marginally stable. The compensated system exhibits better transient and steady-state response. The optimized lead-lag compensated system achieves a maximum percentage overshoot of 12.1% and a settling time of 1.95 sec. This is a substantial improvement compared to the uncompensated system with a maximum % overshoot of 20.5% and a settling time of 2.39 sec. The improved response tends to induce greater damping (ζ) in the compensated system from 0.015 to 0.108 and increases leakage coefficient (K) from $3.38 \times 10^{-12} \text{ m}^3/\text{Pa.s}$ to $24.34 \times 10^{-12} \text{ m}^3/\text{Pa.s}$. Optimized lag-lead compensator ensures stability, responsiveness adapting effectively to dynamic operating conditions of VAPP for aerospace application.

This is an open access article under the [CC BY-SA](https://creativecommons.org/licenses/by-sa/4.0/) license.



Corresponding Author:

Vivek Verma

Department of Mechanical Engineering, Amity School of Engineering and Technology, Amity University

Lucknow, Uttar Pradesh 226018, India

Email: vverma@lko.amity.edu

1. INTRODUCTION

In hydro-mechanical control systems, axial-piston swash-plate design is commonly employed in pressure-controlled pumps to enhance efficiency and performance. Figure 1 depicts a typical pressure-controlled pump employed in hydro-mechanical control systems for power and performance delivery, featuring an axial-piston swash-plate design. The pump control system [1], includes an offset actuator and control actuator at the bottom and top respectively. The offset actuator, exposed to the pump delivery pressure (P_d), works in conjunction with a bias spring to mitigate destroking pressure impacts. Simultaneously, the control actuator modulates the pump stroke proportionally with the control pressure (P_c), regulated by a 3-way hydro-mechanical valve, depicted in Figure 1. The valve adjusts the control pressure and destrokes the pump in response to the pump discharge pressure. As a result, the system aims to maintain

the desired discharge pressure and achieve a steady operating point, fulfilling the pump's control objective. The control system in Figure 1 is an underdamped second-order system with a damping ratio proportional to the pump leakage coefficient K . This ratio reduces overshoot and settling time but adding leakage improves dynamic response while decreasing efficiency. Therefore, a balance between efficiency and dynamic response is essential for optimal pressure-controlled pump performance.

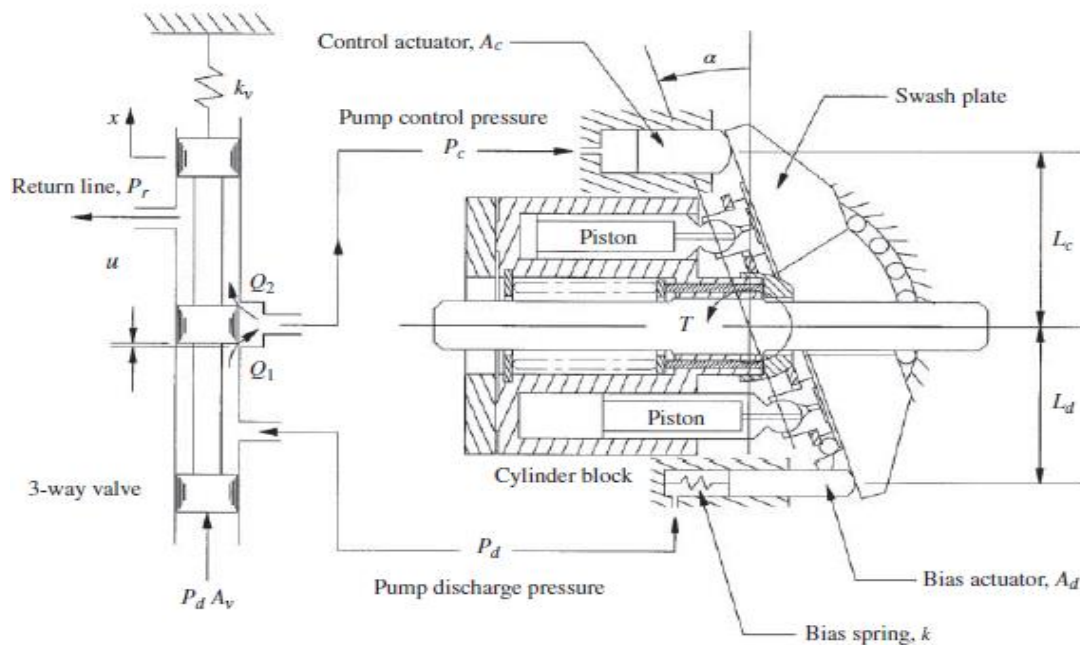


Figure 1. Pressure-controlled axial piston pump [1]

The analysis of optimal control laws, as demonstrated by [2], showcases the efficacy of employing a two-stage valve over a single-stage valve, leading to improved response frequencies and reduced peak pressures, thus indicating superior pump control capability. Building upon this foundation, subsequent research efforts delve deeper into the intricate dynamics of variable displacement pumps. For instance, studies such as [3] emphasize the significant influence of control valve and piston areas on outlet pressure regulation, particularly under varying operating conditions. Moreover, works like [4] provide insights into the importance of static and dynamic characteristics modeling, highlighting the critical role of pump properties in pressure control. As explored in [5], closed-form design equations offer a structured approach to address parameter variations, while investigations into control strategies, including fuzzy logic and nonlinear gain adaptation [6], underscore the potential for enhanced pressure control. Furthermore, research such as [7] emphasizes the importance of optimizing pump-and-valve configurations to improve bandwidth frequency. Expanding on these findings, studies like [8] introduce innovative control strategies tailored to specific pump applications, showcasing robust performance through experimental validation. Additionally, investigations into aeronautical axial piston pumps [9] and variable displacement radial piston pumps [10] shed light on key parameters influencing pump performance and control mechanisms. Furthermore, novel configurations such as the single-actuator setup proposed in [11] address conventional limitations, while research on robust control methods [12] and power control systems [13] offer avenues for improved stability and efficiency. Moreover, advancements in electro-hydraulic systems [14], [15] and mechanical component optimizations [16], [17] further contribute to the evolving landscape of pump control. Notably, efforts focused on vibration control [18], [19] and valve design enhancements [20] underscore the interdisciplinary nature of pump system optimization. Additionally, research on electro-pneumatic proportional systems [21] highlights reliable constant pressure control despite inherent delays in valve mechanisms. Finally, studies like [22], [23] advocate for robust control methodologies, emphasizing their superiority in resilience and precision over traditional proportional-integral-derivative (PID) controllers [24], [25]. The T-SPID controller improves stability and responsiveness, cutting adjustment time by 50% [26]. MATLAB/Simulink simulations identify key parameters for enhancing accuracy and performance [27], [28].

Through ongoing research and development, the field has made significant strides, providing detailed insights and practical solutions for improving pump performance and control across various applications. However, the controllers designed in earlier studies have generally not incorporated compensators to enhance the performance of variable axial piston pumps (VAPP). Most of these studies have focused on optimizing a specific aspect such as reducing pressure fluctuations or maximizing efficiency. There is a clear gap in the development of compensator designs that can optimize pump performance, including minimizing energy consumption, reducing wear and tear, and maintaining high system responsiveness. Thus, the current study sets its objectives based on a thorough review of the existing literature, with recent work summarized in Table 1 as follows:

- To develop dynamic pump model.
- To develop an algorithm for implementing lead-lag compensator for improved VAPP performance.
- To design a controller for the optimum dynamic response of a pressure-controlled swashplate-type axial piston pump.

Table 1. Summary of recent research work

Author name	Year	Reference	Objective	Key findings
Feng <i>et al.</i>	2023	[22]	The study modelled the VAPP and explore robust H _∞ control theory.	Robust H _∞ control, the controller outperformed PID controllers in control precision, and system response time.
Ghosh <i>et al.</i>	2023	[20]	The study optimized a spool valve of VAPP.	Finite element analysis optimized spool design to prevent failure.
Feng <i>et al.</i>	2023	[27]	To develop a mathematical model for APP and evaluate fuzzy control methods for stability and response.	The T-SPID controller has better stability and response, reducing adjustment time 50% compared to traditional methods.
Jiang <i>et al.</i>	2022	[28]	The study analyzes the complex dynamics of electro-hydraulic servo pump systems.	MATLAB/Simulink simulations, identifies key parameter for enhancing system accuracy and performance.
Qian <i>et al.</i>	2021	[26]	Investigated an electro-hydraulic servo system for controlling a hydraulic motor.	Simulations confirmed PID controller's effective speed control, at 60–70 °C, with stable performance under disturbances.
Kumar and Mandal	2021	[10]	Pressure control in a variable displacement radial piston pump (VDRPP) using a PID controller and valve plate design optimization.	An optimized valve plate reduces leakage and enhances efficiency. Simulink analysis confirms effective pressure control and detailed flow behavior in the VDRPP.
Zhao and Huang	2020	[21]	Develop a constant pressure control method using proportional and open-loop technology.	Experiments demonstrate the feasibility of this approach, highlighting its high precision and cost-effectiveness.
Chen <i>et al.</i>	2016	[9]	Developed a model to study pressure drops in an aircraft hydraulic axial piston pump at varying speeds.	They identified pressure drop causes and effects of spool-mass, spring stiffness, and piston count, for improved pump performance.

2. MATHEMATICAL MODELLING AND ANALYSIS OF PRESSURE-CONTROLLED VARIABLE DELIVERY AXIAL PISTON PUMP

The mathematical modeling of the pressure-controlled variable delivery axial piston pump is developed in this section. To accomplish the research objective, the transfer function for the equivalent hydromechanical system of a variable delivery axial piston pump was formulated. The governing equations for the dynamic system were derived by considering the dynamics of the barrel, which influences delivery pressure, the swash plate, which acts as a mechanism to convert rotational motion into reciprocating motion for variable discharge, and the 3-way spool valve.

2.1. Dynamics of delivery pressure

Considering the fundamental pressure-rise-rate equation, factoring in fluid compressibility and instantaneous discharge flow variations, we derive the governing equation for discharge pressure (P_d) [14], [25].

$$\frac{V}{\beta} \dot{P}_d + KP_d = Q - Q_{sys} \tag{1}$$

The model includes V (fluid volume in discharge line), β (bulk modulus), K (pump leakage coefficient), Q (flow rate from pump), and Q_{sys} (flow rate drawn by the downstream system).

For steady-state operating conditions,

$$Q_{sys} = Q_0 - KP_{d_0} \tag{2}$$

where Q_o is average pump discharge and P_{d_0} is average delivery pressure. Replacing this outcome in (1) yields the governing equation for the pump's delivery pressure:

$$\frac{V}{\beta} \dot{P}_d + K(P_d - P_{d_0}) = Q - Q_0 \quad (3)$$

as these pumps maintain a constant angular velocity of the shaft, hence:

$$Q - Q_0 = G_p(\alpha - \alpha_0) \quad (4)$$

where α is pitch plate angle, G_p is pump gain given by,

$$G_p = \frac{NA_p r \omega}{\pi} \quad (5)$$

where N =number of pistons, A_p =piston x-section, r =piston pitch radius, and ω =shaft angular speed. Using (3) and (4) the governing equation becomes,

$$\frac{V}{\beta} \dot{P}_d + K(P_d - P_{d_0}) = G_p(\alpha - \alpha_0) \quad (6)$$

this equation implies that changes in the α can directly influence the discharge pressure P_d .

2.2. Swash plate dynamics

Neglecting the swash plate's dynamics and transient control pressure effects, for incompressible fluid the conservation of mass yield:

$$0 = Q_1 - Q_2 + A_c L_c \dot{\alpha} \quad (7)$$

where Q_1 and Q_2 are the flow rates of the 3-way valve. From 3-way valve analysis,

$$Q_1 - Q_2 = 2K_q x \quad (8)$$

where K_q and x are valve, flow gain and displacement respectively (provided that the $P_c = \frac{1}{2} P_d$). In (7) and (8), gives the governing equation for swash plate dynamics as:

$$\dot{\alpha} = -\frac{K_q}{A_c L_c} x \quad (9)$$

2.3. Valve displacement (x)

The equation of motion of 3-way spool valve:

$$K_v x = A_v P_d + F_x - F_{v_0} \quad (10)$$

where K_v is valve spring rate, A_v is the valve x-sectional area, F_x is the valve flow force, and F_{v_0} is spring preload on the valve at $x=0$. The flow force on the 3-way open-centered valve:

$$F_x = -2K_{f_q} x \quad (11)$$

where K_{f_q} is the valve flow force gain. At the steady operating conditions, the valve spring preload:

$$F_{v_0} = A_v P_{d_0} \quad (12)$$

where P_{d_0} is the desired pump delivery pressure. Combining (11) with design constraints into (10), the equation of motion for the 3-way spool valve will be:

$$x = \frac{A_v}{(K_v + 2K_{f_q})} (P_d - P_{d_0}) \quad (13)$$

2.4. Pressure-controlled axial piston pumps dynamic equations

The equation of motion for the spool valve indicates that adjustments to its position are executed based on the sensed error in the discharge pressure. Utilizing (6), (9), and (13), we can summarize the dynamic equations for the pressure-controlled pump as follows:

$$\dot{P}_d = -\frac{\beta K}{V}(P_d - P_{d_0}) + \frac{\beta G_p}{V}(\alpha - \alpha_0) \tag{14}$$

$$\dot{\alpha} = -\frac{2K_q A_v}{A_c L_c (K_v + 2K_{f_q})}(P_d - P_{d_0}) \tag{15}$$

The characteristic equation for the dynamic system depicted in Figure 2 can be formulated using either state space methods or the Laplace transform.

$$s^2 + as + b = 0 \tag{16}$$

where the coefficients are,

$$a = \frac{K\beta}{V} \quad b = \frac{2K_q A_v G_p \beta}{A_c L_c (K_v + 2K_{f_q}) V} \tag{17}$$

now, the transfer function $G(s)$ of the system can be defined as (18).

$$G(s) = \frac{C(s)}{R(s)} = \frac{b}{s^2 + as + b} \tag{18}$$

Once we have the desired poles, we can design a lead-lag compensator to shift the poles to the desired locations. The lag-lead compensator combines a gain, two poles, and two zeros, mirroring the integration of a lag and lead compensator. Following common electronic implementation [27], its structure is:

$$G_{c_lag_lead}(s) = K_c \frac{1}{\alpha_d} \left(\frac{s+z_{cd}}{s+p_{cd}} \right) * \frac{1}{\alpha_g} \left(\frac{s+z_{cg}}{s+p_{cg}} \right) = K_c \left(\frac{s \tau_d + 1}{s \alpha_d \tau_d + 1} \right) \times \left(\frac{s \tau_g + 1}{s \alpha_g \tau_g + 1} \right) \tag{20}$$

with,

$$\begin{aligned} z_{cd} > 0, p_{cd} > 0, \alpha_d = \frac{z_{cd}}{p_{cd}} < 1, \tau_d = \frac{1}{z_{cd}} = \frac{1}{\alpha_d p_{cd}} \\ z_{cg} > 0, p_{cg} > 0, \alpha_g = \frac{z_{cg}}{p_{cg}} > 1, \tau_g = \frac{1}{z_{cg}} = \frac{1}{\alpha_g p_{cg}} \end{aligned} \tag{21}$$

the subscript d indicates the lead compensator, and the subscript g indicates the lag compensator.

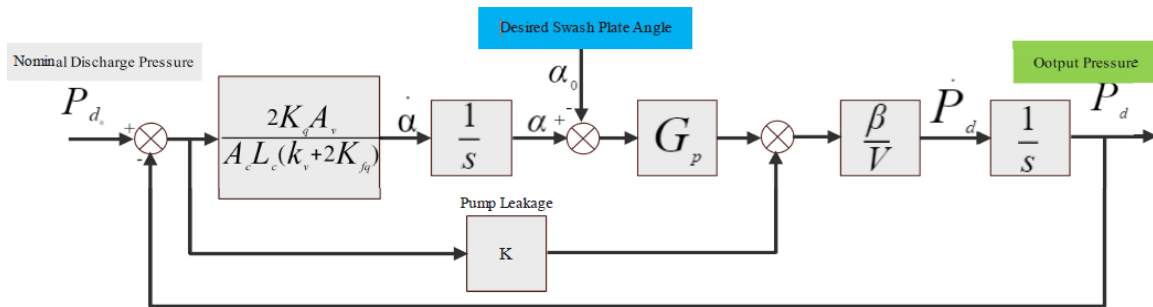


Figure 2. Schematic diagram of the hydro-mechanical control system

2.5. Algorithm: lead-lag compensation design for pressure-controlled axial piston pumps

Lead-lag compensation enhances stability and response in pressure-controlled axial piston pumps by adjusting phase and gain. This algorithm designs a lead-lag compensator for a variable delivery pump to improve transient response, reduce steady-state error, and ensure precise pressure control.

```

Inputs:
Steady-state error (SSE) ess_specified;
Phase margin (PMspecified);
Gain x-over frequency ωx.
Plant Transfer function: G(s) = b / (s2 + as + b), 'a' and 'b' are parameters of the plant
Outputs:
Transfer function of the lag-lead compensator
Procedure:
1. Increase System Type (if necessary):
   Augment system with required poles at s = 0 to meet SSE specs:
    
```

$$G_{augmented}(s) = K_c G_p(s) / s^{(N_{req} - N_{sys})}$$

Compute K_c for steady-state error

2. Generate Bode Plots:

Plot $G_{augmented}(s)$ to analyze system dynamics.

3. Design Lead Compensator:

Compute phase shift at specified gain crossover frequency ω_x : $\varphi = \arg [G_{augmented}(j\omega_x)]$

Compute the uncompensated phase margin $PM_{uncompensated}$

$$PM_{uncompensated} = 180^\circ + \angle G(j\omega_x)$$

Compute parameters for desired phase margin:

$$\varphi_{max} = PM_{specified} + 10^\circ - PM_{uncompensated}$$

$$\alpha_d = \frac{1 - \sin(\varphi_{max})}{1 + \sin(\varphi_{max})}$$

Compute lead compensator's zero and pole: $z_{cd} = \omega_x \sqrt{\alpha_d}$, $p_{cd} = \frac{z_{cd}}{\alpha_d}$

4. Design Lag Compensator:

Determine magnitude at specified gain crossover frequency ω_x : $G_{augmented}(j\omega_x)$

Compute attenuation required for desired gain margin: $\alpha_g = \frac{1}{|G_{lead}(j\omega)G_p(j\omega)|_{db}}$

Compute lag compensator's zero and pole: $z_{cg} = \frac{\omega_{specified}}{10}$, $p_{cg} = \frac{z_{cg}}{\alpha_g}$

5. Implementation:

Choose resistor and capacitor values for compensator design.

Output:

The designed lag-lead compensator meets specified input parameters criteria.

End Algorithm

2.6. Lead-lag compensator implementation

Ogata [29] discussed implementations of analog circuit for all types of compensators. The lead-lag compensator circuit uses two inverting operational amplifiers in series to adjust phase and magnitude effectively. The first amplifier's input impedance designed as resistor R_1 in series with capacitor C_1 , in parallel with resistor R_3 . The feedback impedance is defined as resistor R_2 in series with capacitor C_2 , and in parallel with resistor R_4 . The second amplifier is designed with input resistors R_5 and feedback R_6 . Assuming that the output amps are ideal, the transfer function for this circuit is:

$$\frac{V_{out}(s)}{V_{in}(s)} = \left. \begin{aligned} & \frac{R_6 R_4 [s(R_3 + R_3)C_1 + 1] (sR_2 C_2 + 1)}{R_5 R_3 (sR_1 C_1 + 1) [s(R_2 + R_4)C_2 + 1]} \\ & \frac{R_6 R_4}{R_5 R_3} \cdot \frac{R_2(R_1 + R_3)}{R_1(R_2 + R_4)} \cdot \frac{(s + \frac{1}{(R_1 + R_3)C_1})}{(s + \frac{1}{R_1 C_1})} \cdot \frac{(s + \frac{1}{R_2 C_2})}{(s + \frac{1}{(R_2 + R_4)C_2})} \end{aligned} \right\} \quad (22)$$

comparing the (22) and (20), we get,

$$\left. \begin{aligned} K_c &= \frac{R_6 R_4}{R_5 R_3}, z_{cd} = \frac{1}{(R_1 + R_3)} C_1, p_{cd} = \frac{1}{R_1 C_1}, \alpha_d = \frac{R_1}{R_1 + R_3} \\ z_{cg} &= \frac{1}{R_2 C_2}, p_{cg} = \frac{1}{(R_2 + R_4)C_2}, \alpha_g = \frac{R_2 + R_4}{R_2} \end{aligned} \right\} \quad (23)$$

3. RESULTS AND DISCUSSION

In the design of a feedback control system, targeting a phase margin of 30–60 degrees and a gain margin of 2–10 dB is key to optimal stability and response [30]. Large margins yield stability but slow response, while small margins offer quicker response but may induce oscillation. Balancing these margins is key to maximizing system performance [31].

Employing the data from the Table 2 transfer function for the second-order underdamped system is,

$$G(s) = \frac{10000}{s^2 + 3s + 10000} \quad (24)$$

By using the algorithm illustrated in section 2.5, the transfer function of the designed lead-lag compensator depicted in Figure 3 with specification is given as:

$$G_{c \text{ lead-lag-compensator}} = \frac{27.3 \cdot (s + 1.34)(s + 1)}{s \cdot (s + 18.66)(s + 0.39)} = \frac{27.3 \cdot (s^2 + 2.34s + 1.34)}{(s^3 + 18.7s^2 + 0.73s)} \quad (25)$$

$$G_{c \text{ lead-lag-compensator}} G_p(s) = \frac{10000 \cdot 27.3 \cdot (s^2 + 2.34s + 1.34)}{(s^2 + 3s + 10000)(s^3 + 18.7s^2 + 0.73s)} \quad (26)$$

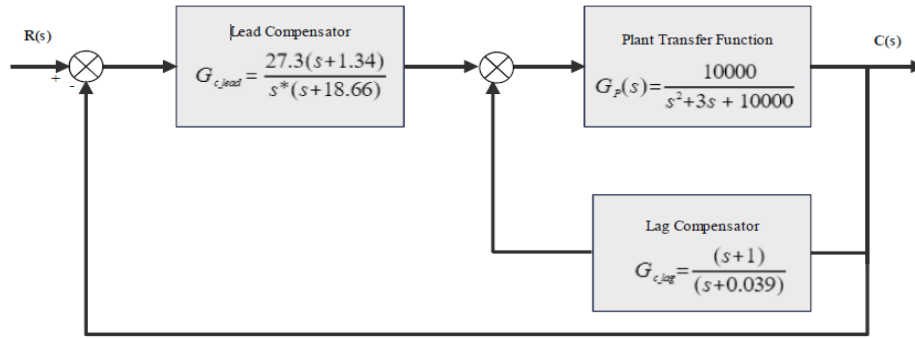


Figure 3. Block diagram of the lead-lag compensator

The bode plots in Figure 4 and step responses in Figures 5 to 9 of the uncompensated and compensated system are drawn using MATLAB version R2023b for academic use. Analysing the results depicted in Figures 4 to 9 summarized in Table 3 indicates that the basic plant $G_p(s)$ has a phase margin of 24.5° , a gain crossover frequency of 3.38 rad/s, and a moderate performance with a settling time of 2.39 seconds and 20.5% overshoot. The lead compensation provides a good balance, achieving a phase margin of 40.4° and a gain crossover frequency of 30 rad/s, though it has a longer time delay of 1.1 seconds. In contrast, the proportional control is unstable, with the highest overshoot of 60%, the longest settling time of 7.42 seconds, and an unstable gain margin. The lag-lead compensated system offers the best overall results, with the highest phase stability margin of 55.7° , low overshoot of 12.1%, and the fastest settling time of 1.95 seconds.

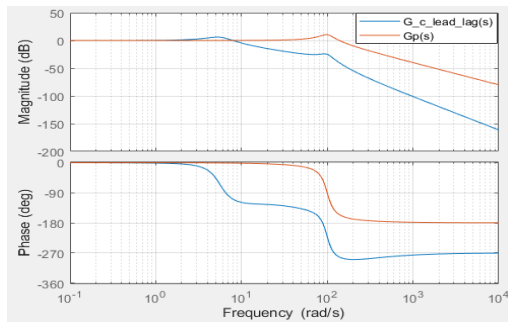


Figure 4. Bode plot for uncompensated and compensated systems

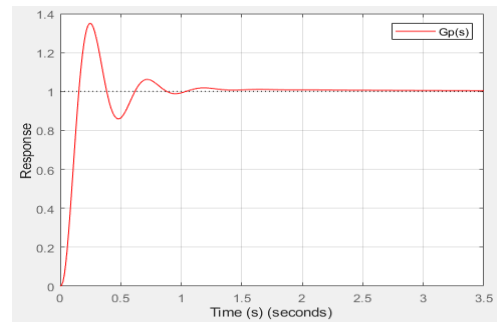


Figure 5. Closed loop step response of the $G_p(s)$

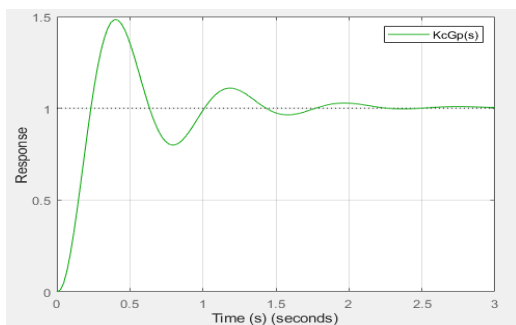


Figure 6. Closed loop step response of the $K_c G_p(s)$

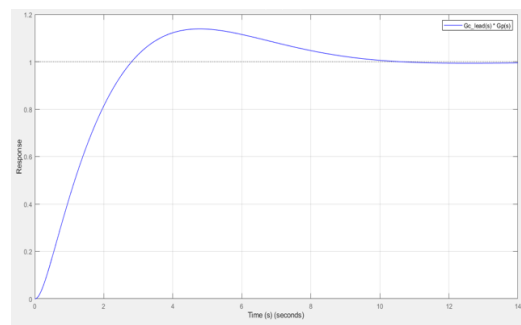


Figure 7. Closed loop step response of the $G_{c_lead} * G_p(s)$

The optimized lead-lag compensator offers better transient response and steady-state error specified in input design parameters. The uncompensated system is marginally stable having a higher steady-state error of 1 while the compensated system ensures robust control with enough phase margins of 55.7° and gain

margins of 12.3 dB along with a low steady-state error of 0.02. The control system in a closed loop with unity feedback employing a lead-lag compensator along with the plant in series meets all the specifications.

The bode plot in Figure 4 satisfies the specified input design parameters of a lead-lag compensator. Analyzing the step responses of various systems clearly shows a lead-lag compensated system has a smaller settling time of 1.95 sec, reduced overshoot of 12.1%, and much better stability margins than the $G_p(s)$. Comparing the result obtained in the study with H_∞ controller [22], [23] the lag-lead compensator offers a much better balance between stability and response speed for a pressure-controlled system, while H_∞ control is particularly beneficial for enhancing response speed and efficiency in servo control systems. The designed lead-lag compensator $G_{c_lag_lead}(s)$, can be implemented with the values given in Table 4, computed from (23).

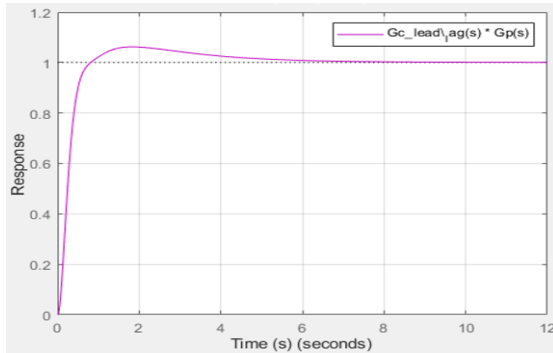


Figure 8. Closed loop step response of the $G_{c_lead_lag} * G_p(s)$

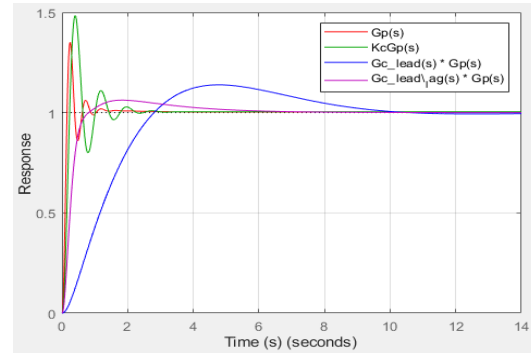


Figure 9. Closed loop step responses

Table 2. The pressure-controlled pump parameters

Parameter	Value	Parameter	Value	Parameter	Value
V_p	45 cm ³ /rev	G_p	4.15×10 ⁻³ m ³ /s	K	3.38×10 ⁻¹² m ³ /Pa. s
P_d	25 MPa	A_c	3.76 cm ²	β	0.8 Gpa
N	1800 rpm	L_c	6.75 cm	V	30 litres
K_q	0.19 m ² /s	K_{fq}	5.76 N/mm	K_v	56.55 N/mm
A_v	28.77 mm ²	$e_{ss\text{speci}}$	0.02	PM_{speci}	>55°
ω_x	8 rad/s				

Table 3. Comparison Between Systems

Control parameters	Notation	$G_p(s)$	$K_c * G_p(s)$	$G_{c_lead}(s) * G_p(s)$	$G_{c_lag_lead}(s) * G_p(s)$
SSE	e_{ss}	1	0.02	0.02	0.02
Phase stability margin	ϕ_m	24.5°	15.5°	40.4°	55.7°
Gain x-over freq	ω_x	3.38 rad/s	15 rad/s	30 rad/s	7.82 rad/s
Time delay	t_d	0.025 sec	0.016 sec	1.1 sec	0.18 sec
Gain margin (db)	GM (db)	inf	Unstable	11.6 dB	12.3 dB
Phase x-over freq	ω_ϕ	inf	100 rad/s	93.4 rad/s	88 rad/s
Frequency bandwidth	ω_b	170.5 rad/s	170.5 rad/s	163.8 rad/s	161.47 rad/s
% overshoot	MPO	20.5%	60%	15%	12.1%
Settling time	t_s	2.39 sec	7.42 sec	3.16 sec	1.95 sec
Damping factor	ζ	0.015	0.015	0.093	0.108

Table 4. Implementation results of lead-lag compensator

Circuit elements	Values	Circuit elements	Values	Circuit elements	Values
C_1	0.2 μ F	R_1	37.3 M Ω	R_4	1.28 G Ω
C_2	0.2 μ F	R_2	50 M Ω	R_6	3.77 M Ω
R_5	20 K Ω	R_3	4.82 G Ω		

Where C_1 , C_2 , and R_5 have specified values.

4. CONCLUSION

This study aimed to enhance the dynamic performance of the pressure-controlled VAPP by implementing the lead-lag compensator while developing a mathematical model of the pump, taking into account the dynamics of the barrel, 3-way spool valve, and swash plate. The developed control system with

lag-lead compensator of the pressure-controlled axial piston pump manifests the characteristics of an underdamped second-order system, distinguished by inherent properties such as natural frequency and damping ratio. The damping ratio, integral to the pump leakage coefficient (K), plays a pivotal role in regulating both the maximum percent overshoot and the settling time of the system's dynamic response, has shown significant improvement from the uncompensated system to compensated system reflected in the results. The compensated system enhanced the damping factor from 0.015 to 0.108, which tends to increase the leakage coefficient (K) from $3.38 \times 10^{-12} \text{ m}^3/\text{Pa} \cdot \text{s}$ to $24.34 \times 10^{-12} \text{ m}^3/\text{Pa} \cdot \text{s}$. This increase in leakage tends to induce better transient and steady-state response in the compensated system with lower settling time from 2.39 sec to 1.95 sec and SSE from 1 to 0.02. However, this deliberate introduction of leakage tends to enhance the pump's responsiveness, it simultaneously imposes a trade-off by diminishing the overall operational efficiency of the VAPP.

In conclusion, the lag-lead compensated system demonstrates superior performance, achieving the highest phase margin (55.7°), lowest overshoot (12.1%), and fastest settling time (1.95 seconds), making it the most effective control strategy than the H_∞ controller. Striking a prudent equilibrium between efficiency and dynamic response is a critical aspect in designing a pressure-controlled pump system suited to specific aerospace applications. This aspect underscores the rationale behind the adoption of a lag-lead compensator, which facilitates the optimization of system performance while addressing the inherent trade-offs between efficiency and dynamic response. Future work should concentrate on advanced control techniques, incorporating real-time testing, and exploring predictive methods like adaptive model predictive control. Improving robustness and tailoring strategies for specific aerospace applications will further enhance system stability, response, and overall performance.

REFERENCES

- [1] N. D. Manring and R. C. Fales, *Hydraulic control systems*. John Wiley & Sons, 2019.
- [2] S. J. Lin and A. Akers, "Optimal control theory applied to pressure-controlled axial piston pump design," *Journal of Dynamic Systems, Measurement, and Control*, vol. 112, no. 3, pp. 475–481, Sep. 1990, doi: 10.1115/1.2896167.
- [3] D. McCandlish and R. E. Dorey, "The mathematical modelling of hydrostatic pumps and motors," *Proceedings of the Institution of Mechanical Engineers, Part B: Journal of Engineering Manufacture*, vol. 198, no. 3, pp. 165–174, 1984, doi: 10.1243/PIME_PROC_1984_198_062_02.
- [4] P. Kaliafietis and T. Costopoulos, "Modelling and simulation of an axial piston variable displacement pump with pressure control," *Mechanism and Machine Theory*, vol. 30, no. 4, pp. 599–612, May 1995, doi: 10.1016/0094-114X(94)00057-R.
- [5] N. D. Manring and R. E. Johnson, "Modeling and designing a variable-displacement open-loop pump," *Journal of Dynamic Systems, Measurement, and Control*, vol. 118, no. 2, pp. 267–271, Jun. 1996, doi: 10.1115/1.2802313.
- [6] D. Lovrec and E. Detiček, "Improvement of the statical behaviour of pressure controlled axial piston pumps," *Strojnikski Vestnik/Journal of Mechanical Engineering*, vol. 55, no. 12, pp. 766–774, 2009.
- [7] N. D. Manring and V. S. Mehta, "Physical limitations for the bandwidth frequency of a pressure controlled, axial-piston pump," *Journal of Dynamic Systems, Measurement and Control, Transactions of the ASME*, vol. 133, no. 6, p. 061005, 2011, doi: 10.1115/1.4004056.
- [8] W. Kemmetmüller, F. Fuchshumer, and A. Kugi, "Nonlinear pressure control of self-supplied variable displacement axial piston pumps," *Control Engineering Practice*, vol. 18, no. 1, pp. 84–93, 2010, doi: 10.1016/j.conengprac.2009.09.006.
- [9] L. Chen, S. Ye, Z. Chang, X. Gou, and K. Sun, "Simulation research on the revolution-pressure performance of an aeronautical hydraulic axial piston pump," in *2016 IEEE International Conference on Aircraft Utility Systems (AUS)*, Oct. 2016, pp. 1247–1251, doi: 10.1109/AUS.2016.7748230.
- [10] L. Kumar and N. P. Mandal, "Pressure control of variable displacement radial piston pump with PID controller," *Materials Today: Proceedings*, vol. 45, no. 6, pp. 5158–5165, 2021, doi: 10.1016/j.matpr.2021.01.692.
- [11] Hongliu Du and N. D. Manring, "A single-actuator control design for hydraulic variable displacement pumps," in *Proceedings of the 2001 American Control Conference. (Cat. No.01CH37148)*, 2001, vol. 6, pp. 4484–4489, doi: 10.1109/ACC.2001.945685.
- [12] P. T. Dean and R. C. Fales, "Modern control design for a variable displacement hydraulic pump," in *2007 American Control Conference*, Jul. 2007, pp. 3535–3540, doi: 10.1109/ACC.2007.4282826.
- [13] O. Gad, M. G. Rabie, and R. M. El-Taher, "Prediction and improvement of steady-state performance of a power controlled axial piston pump," *Journal of Dynamic Systems, Measurement, and Control*, vol. 124, no. 3, pp. 443–451, Sep. 2002, doi: 10.1115/1.1485096.
- [14] S. H. Park, J. M. Lee, and J. S. Kim, "Modeling and performance improvement of the constant power regulator systems in variable displacement axial piston pump," *The Scientific World Journal*, vol. 2013, no. 1, Jan. 2013, doi: 10.1155/2013/738260.
- [15] P. Achten, "Dynamic high-frequency behaviour of the swash plate in a variable displacement axial piston pump," in *Proceedings of the Institution of Mechanical Engineers, Part I: Journal of Systems and Control Engineering*, Jul. 2013, vol. 227, no. 6, pp. 529–540, doi: 10.1177/0959651813483419.
- [16] J. Wei, K. Guo, J. Fang, and Q. Tian, "Nonlinear supply pressure control for a variable displacement axial piston pump," *Proceedings of the Institution of Mechanical Engineers, Part I: Journal of Systems and Control Engineering*, vol. 229, no. 7, pp. 614–624, Aug. 2015, doi: 10.1177/0959651815577546.
- [17] J. Cheng, W. Liu, and Z. Zhang, "Modeling and simulation for the electro-hydraulic servo system based on Simulink," in *2011 International Conference on Consumer Electronics, Communications and Networks (CECNet)*, Apr. 2011, pp. 466–469, doi: 10.1109/CECNET.2011.5768860.
- [18] K. Guo, Y. Xu, and J. Li, "A switched controller design for supply pressure tracking of variable displacement axial piston pumps," *IEEE Access*, vol. 6, pp. 3932–3942, 2018, doi: 10.1109/ACCESS.2018.2796097.
- [19] T. Kim and M. Ivantysynova, "Active vibration/noise control of axial piston machine using swash plate control," Oct. 2017, doi: 10.1115/FPMC2017-4304.

- [20] A. Ghosh, A. Gupta, and N. Mondal, "Design and design investigations of a flow control spool valve," *International Journal on Interactive Design and Manufacturing (IJIDeM)*, vol. 17, no. 1, pp. 115–124, Feb. 2023, doi: 10.1007/s12008-022-01135-1.
- [21] T. Zhao and D. Huang, "Research and implementation of constant pressure control with electro-pneumatic proportional valve," *Journal of Physics: Conference Series*, vol. 1626, no. 1, p. 012075, Oct. 2020, doi: 10.1088/1742-6596/1626/1/012075.
- [22] Y. Feng, Z. Jian, J. Li, Z. Tao, Y. Wang, and J. Xue, "Advanced control systems for axial piston pumps enhancing variable mechanisms and robust piston positioning," *Applied Sciences*, vol. 13, no. 17, p. 9658, Aug. 2023, doi: 10.3390/app13179658.
- [23] D. Satybalidina, A. Dabayeva, N. Kissikova, G. Uskenbayeva, and A. Shukirova, "Mixed H_2/H_∞ robust controllers in aircraft control problem," *International Journal of Electrical and Computer Engineering (IJECE)*, vol. 13, no. 6, pp. 6249–6258, Dec. 2023, doi: 10.11591/ijece.v13i6.pp6249-6258.
- [24] S. Albatran and S. Harasis, "Optimal proportional-integral speed control for closed-loop engine timing system," *Indonesian Journal of Electrical Engineering and Computer Science (IJECS)*, vol. 34, no. 1, pp. 128–133, Apr. 2024, doi: 10.11591/ijeecs.v34.i1.pp128-133.
- [25] J. Ivantysyn and M. Ivantysynova, "Analysis of an axial-piston swash-plate type hydrostatic pump discharge flow characteristic," in *Hydrostatic Pump and Motors: Principles, Design, Performance, Modelling, Analysis, Control and Testing*, Tech Books International, 2003.
- [26] S. Qian, W. Zhang, and Q. Li, "Design and analysis of electro-hydraulic proportional valve flow control based on fuzzy PID," *Chinese Journal of Construction Machinery*, vol. 19, pp. 512–517, 2021, doi: 10.1109/CAIDCD.2010.5681934.
- [27] Y. Feng, Z. Jian, and L. I. Jia-yang, "Axial piston pump variable mechanism control strategy," *Chinese Hydraulics & Pneumatics*, vol. 47, no. 3, pp. 9–16, 2023, [Online]. Available: <http://journal.cmanu-automation.cn/yyyqd/EN/10.11832/j.issn.1000-4858.2023.03.002>.
- [28] W. Jiang *et al.*, "A study on the electro-hydraulic coupling characteristics of an electro-hydraulic servo pump control system," *Processes*, vol. 10, no. 8, p. 1539, Aug. 2022, doi: 10.3390/pr10081539.
- [29] K. Ogata, *Modern control engineering*. Prentice Hall, 2010.
- [30] S.-H. Kim, "Control of direct current motors," in *Electric Motor Control*, Elsevier, 2017, pp. 39–93.
- [31] L. Danes and A. Vacca, "A frequency domain-based study for fluid-borne noise reduction in hydraulic system with simple passive elements," *International Journal of Hydromechanics*, vol. 4, no. 3, pp. 203–229, 2021, doi: 10.1504/IJHM.2021.118006.

BIOGRAPHIES OF AUTHORS



Vivek Verma     is a part-time research scholar at the Department of Mechanical Engineering at Amity School of Engineering and Technology, Amity University, Lucknow. He holds B.E. in Industrial Engineering from IIT Roorkee (formerly University of Roorkee), India and M.Tech. in Production Engineering from MNNIT, Allahabad, India. Currently he is working as Assistant Professor at Department of Mechanical Engineering, ASET, Amity University, Lucknow, has vast experience of teaching about 20 years. He used to hold several administrative posts at the Department and University levels. He is a member of several professional bodies such as SAE, IET(UK), and IAENG. He has supervised 10 masters and more than 50 undergraduate students. He has organized several FDP consultancy projects as well. He has research interest in mathematical modelling of mechanical systems and computational fluid dynamics. He can be contacted at email: vverma@lko.amity.edu.



Dr. Sachin Kumar     a Ph.D. in Electronics, M.Tech. and B.E in Electronics and Communication, presently with Amity University, Lucknow Campus. He has almost 20 years of academic and research experience. His research interest includes applications of bio-medical signal processing, machine learning, artificial intelligence and applications of wireless sensor networks. He is an active member of number of professional bodies IEEE, IETE, IAENG, ISC and IET(UK), he has published more than 80 research papers, book chapters, and articles in a number reputed Journals indexed in SCOPUS and SCI and contributed 2 books with international publishers. He is an active member of editorial board/reviewer in various reputed journals. He has been instrumental in organizing number of international conferences, has given invited talks, and chaired various technical sessions in national as well as international conferences of repute. He can be contacted at email: skumar3@lko.amity.edu.



Dr. Apurva Anand     currently holds the position of Professor and Director at Maharana Pratap Engineering College, Kanpur, showcasing a career spanning over two dynamic decades. In his previous role, he served as the Professor and Dean at BBD University in Lucknow from 2017 to 2023. His academic journey includes key roles at renowned institutions, notably ABES Engineering College and Amity University, where he served as Professor and Head of the Department. Holding a Ph.D. in Mechanical Engineering and Master's in Mechanical Engineering and a Bachelor's in Industrial and Production Engineering. He scholarly impact is evident in his 30 publications, garnering 401 citations and achieving an impressive h-index of 05. In the realm of global collaboration, he served as Program Chair for several international conferences, his contributions extend to funded assignments, including a University Grant for organizing a FDP on Manufacturing Science and Technology. Actively guiding one Ph.D. scholar 10 PG students. He can be contacted at email: director.mpec@mpgi.edu.in or apurva2050@yahoo.co.in.